HOURLY GLOBAL RADIATION PREDICTION FROM GEOSTATIONARY SATELLITE DATAHOURLY GLOBAL RADIATION PREDICTION FROM GEOSTATIONARY SATELLITE DATA

Pierrick Haurant, Cyril Voyant, Marc Muselli, Marie Laure Nivet, Christophe Paoli

HAL Id: hal-00865919

https://hal.science/hal-00865919

Submitted on 25 Sep 2013

HOURLY GLOBAL RADIATION PREDICTION FROM GEOSTATIONARY SATELLITE DATA

Pierrick Haurant[1,2*], Cyril Voyant[3,4], Marc Muselli[4], Marie-Laure Nivet[4] and Christophe Paoli[4]
[1]Centre Thermique de Lyon (CETHIL), UMR CNRS 5008 / INSA Lyon / UCB Lyon 1, LYON, FRANCE
[2]Chaire INSA/EDF « Habitats and Energy Innovations », LYON, FRANCE
[3]Castelluccio Hospital, Radiophysics Unit, BP 85, 20177 AJACCIO, FRANCE
[4]Université de Corse, UMR CNRS 6134 SPE, 20250 CORTE, FRANCE

ABSTRACT: The possibility to generate 2-D predictions of solar radiation one hour ahead and over a large geographic area is the focus of this study. In that view, hourly satellite maps of irradiations extracted from the Heliosat-3 have been used as training data and inputs of artificial neural networks (ANN) and as inputs for apersistence model. These models were computed for each point of the map, allowing generating solar radiation predictions maps. Comparisons between the computed maps and satellite estimations ones were proceed to evaluate the performances. The first results show that ANN and persistence have similar performances in a majority of pixel.
Keywords: solar radiation, forecast, satellite, maps

1 INTRODUCTION

Intermittency nature of global radiation limits the photovoltaic (PV) systems integration on electrical grids. Indeed, fluctuations of the solar resource lead to strong variations of PV production that can destabilize the electrical network, in case of high integration rate of PV. To overcome this problem, complementary power devices can bridge PV power failures. However, a good management of these different power sources needs predictions of load and fatal intermittent productions, such as PV one, to drive transitions between the different power sources [1,2]. That why surface solar irradiation (SSI) predictions, among others, are of interest for electrical network managers.

Prediction tools that are developed until now use a measured time series for punctual location in Corsica [1,3,4]. This 1-D approach becomes obsolete for the large electrical networks with many spatially dispersed photovoltaic plants. In this paper we introduce a new 2-D prediction tool combining satellite solar radiation estimations and stochastic models.

1 STUDIED AREA

Corsica is a Mediterranean island located in the golf of Genoa. It stretches out on 183 km long between latitudes 41° 20' 02" N and 43° 01' 31" N and 83.5 km wide between longitudes 8° 32' 30" E and 9° 33' 38" E extending to an area of 8722 km².

Corsica were described as a "mountain in the sea" as mountain occupies an important area : 39 % of the surface rise over 600 m while the mean elevation hits 568 m and 120 summits are over 2000 m [5] (Fig. 1).
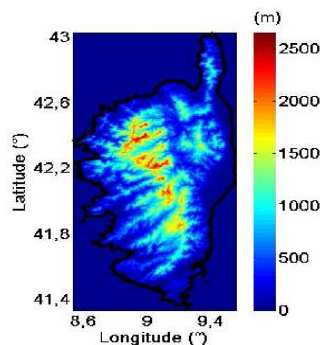

Figure 2: Topography of Corsica from the Digital Elevation Model SRTM3 [6]

The island's seaside globally benefits from a Mediterranean climate characterized by hot dry summers and mild wet winters. It presents one of the greatest solar potential of metropolitan France. The mountainous inner has a climate of height elevations or even alpine climate : summers are hot and sunny but the precipitations are more abundant on winters.

3 SATELLITE DERIVATE HOURLY RADIATION

In Corsica, the public meteorological network is composed of only 6 stations. Only three of them provide hourly radiations measurements while the others provide 10 days integrated data [7]. In that context, 1D predictions can be realized for three punctual locations in Corsica, not enough to allow a global management of electrical network and the photovoltaic plants. Thus, prediction map obtained from SSI maps can represent a good alternative.

Many methods allow a precise knowledge of spatial distribution and temporal behavior of SSI over a territory. Among these methods, remote sensing tools provide satellite derivate SSI of which accuracy has usually been demonstrated. That is why SSI used in this study was extracted from a Helioclim-3 (HC-3) SSI database [6]. This database was selected among the numerous others firstly because it provides 1 hour wise SSI maps during a long period, from 2005 until now, enough to train our predictors. Secondly, the maps have a good nadir spatial resolution 2.5 km, for high resolution predictions. Finally, the accuracy of SSI estimations have been proved [8]..

2.1 Heliosat-2 model

The maps are obtained from Meteosat Second Generation images treated by the Heliosat-2 model [8]. This model use calibrated satellite images that are converted into irradiation as input. Since they result from radiation-surface-atmosphere interactions, a fluctuation of the signal measured by the sensors is interpreted as a variation of the cloud cover. Then, the aim principle of Heliosat-2 consists in considering the SSI derivate from the clear sky radiation multiplied by a cloud index $n_t(i, j)$ that express the cloud cover conditions of the atmosphere

above a pixel i, j at time t :

$$n_t(i,j) = \frac{\rho_t(i,j) - \rho_t^{Cls}(i,j)}{\rho_t^{Cloud}(i,j) - \rho_t^{Cls}(i,j)}$$

In this equation,
- $\rho_t(i,j)$ is the reflectance (or apparent albedo) measured by the sensor;
- $\rho_t^{Cloud}(i,j)$ is the apparent albedo of the brightest clouds calculated,
- $\rho_t^{Cls}(i,j)$ is the apparent albedo of the ground under clear sky.

Then, the clear sky index $k_t^{Cls}(i,j)$ is linked to the cloud index by the following system [7]:

$$\begin{cases} k_t^{Cls}(i,j) = 1.2 \text{ if } n_t(i,j) < -0.2 \\ k_t^{Cls}(i,j) = 1 - n_t(i,j) \text{ if } -0.2 \leq n_t(i,j) < 0.8 \\ k_t^{Cls}(i,j) = 2.0667 - 3.6667 n_t(i,j) \\ \quad +1.6667 n_t(i,j)^2 \text{ if } 0.8 \leq n_t(i,j) < 1.1 \\ k_t^{Cls}(i,j) = 0.05 \text{ if } n_t(i,j) \geq 1.1 \end{cases}$$

Once the clear sky index determined, the global radiation $G_t(i,j)$ is obtained by

$$G_t(i,j) = k_t^{Cls}(i,j) G_t^{Cls}(i,j)$$

where $G_t^{Cls}(i,j)$ designs the global radiation under clear sky condition. Its model, developed in the framework of the European Solar Radiation Atlas (ESRA model) is presented in [10].

In the present study, 1158 points of the HelioClim-3 mesh grid that cover Corsica, covering a period of 8 year between 2005 and 2012, are considered (Fig. 2).
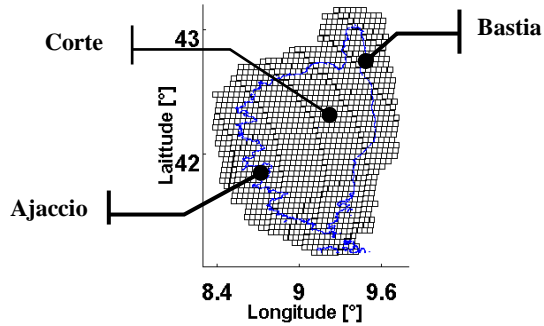
Figure 2: HelioClim-3 mesh grid and meteorological stations location (Black Circles): Ajaccio (41°55'N ; 8°44'E ; 0 m), Corte (42°18'N ; 9°09'E ; 360 m) and Bastia (42°42'N ; 9°27'E ; 0 m)

2.2 Performances of satellites SSI estimations

The performances of those satellite derivate SSI estimations have been evaluated in the case of Corsica, in terms of normalized Mean Bias Error (nMBE, [%]), normalized Root Mean Square Error (nRMSE, [%]) and correlation coefficients CC. In that view, they have been compared to hourly pyranometrical measurements provided by three meteorological stations in Corsica (Fig. 1) that cover the period from April 1st, 2004 to December 17th, 2006.

Table I: Performances of HelioClim-3 satellite estimations over Ajaccio, Bastia and Corte.

	Ajaccio	Bastia	Corte
nRMSE [%]	19.8	23.5	22.0
nMBE [%]	-5.3	-8.27	-2.96
CC	0.98	0.97	0.97

The performances of SSI estimations over these three stations are summed up in table 1. We can note that the estimations are correlated to the measurements since CC are over 0.97. The biases used to be <0 showing that the radiations are underestimated. Finally yearly nRMSE are between 19.8.3 and 23.5 %, lightly over the nRMSE of Meteosat-8 estimations, the satellite derivate SSI maps of MeteoFrance, for the same stations, at the same period [2,5]. However, Meteosat-8 maps have a lower resolution and the data set doesn't cover a so long period than HelioClim-3.

We can anticipate that these performances will be a strong artifact for accurate predictions, but the main objective of this study is to prospect the feasibility of such prediction, knowing that the challenge of more accurate and higher resolution SSI maps will be taken up.

4 PREDICTION MODELS

Several prediction approaches have been developed. They can be divided in two main groups: methods using mathematical formalism of times series (TS) and numerical weather prediction models. TS formalism is based on a linear or non-linear function f_n :

$$\hat{x}_{t+1} = f_n(x_t, \dots, x_{t-p}) + \varepsilon_t$$

where x_t is a TS and p represents the number of lags.

In this study, two functions will be applied to SSI maps: persistences and Artificial Neural Networks (ANN). These models will be applied to SSI of each pixel of the maps (Fig. 3).
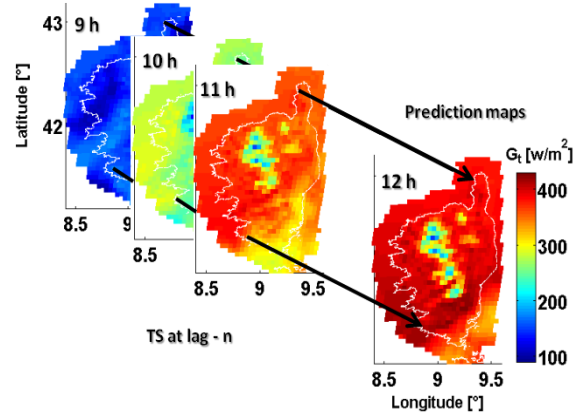
Figure 3: Schematic representation of map prediction

3.1 Persistence

Persistence is a naïve model which principle is to assume that conditions at time $t+1$ are the same than at time t:

$$\hat{x}_{t+1} = x_t$$

Since global radiation in clear sky conditions can be computed with a good accuracy at any time, only the clear sky index will be predict by a persistence. What we call a scaled persistence. Thus,

$$\hat{G}_{t+1}(i,j) = k_t^{Cls}(i,j) G_{t+1}^{Cls}(i,j) = \frac{G_t(i,j)}{G_t^{Cls}(i,j)} G_{t+1}^{Cls}(i,j)$$

3.2 Artificial Neural Networks

ANN are models from artificial intelligence which the concept is inspired on biological neurons : they are constituted by a set of functional interconnected unities called formal neurons. These neurons can be summed up as mathematic functions calculating a weighted sum of the inputs and biases that pass through an activation function f. Thus, considering neuron i of layer n with its ne inputs x_i, the weights $w_{i,j}^n$ and biases b_j, the output y_i is calculated by :

$$y_i = f \left(\sum_{j=1}^{ne} x_i w_{i,j}^n + b_j \right)$$

Although a large amount of different architectures of ANN is exists, MultiLayer Perceptron (MLP) remains the most popular for radiation forcasting [11].
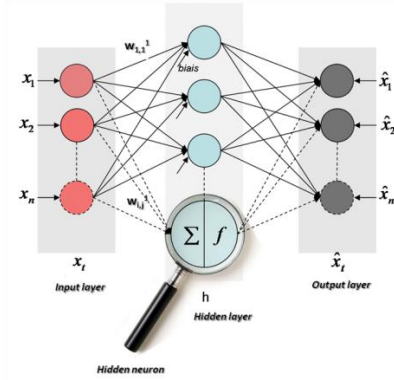

Figure 4: Schematic representation of MLPArtificial Neural Network with one hidden layer

MLP are organised by layers, the information circulate from an input layer to an output one passing in hidden neural (Fig. 4). Actually, feed-forward MLP networks with two layers (one hidden layer and one output layer) are often used.

5   FIRST RESULTS

In the presented study, the MLP were computed with the Matlab© software and its Neural Network toolbox. Their characteristic were defined from [1,10,11]: the ANN used here were made of one hidden layer which neurons activation function is a hyperbolic tangent. The output neuron activation function is linear. The training algorithm is the Levenberg-Marquardt one.

The 6 first years of the radiations maps have been used for the construction of ANN that is based on three steps: training, validation and testing. The number of lags used as inputs was determined from autocorrelations. 5 to 7 lags were used, according to each pixel.

Comparisons between satellite estimated SSI maps and predictions are proceed. In that view, the last 2 years of the available dataset are used to estimate the performances of predictions. Note that the persistence model were applied to the last 2 years too, in order to compare the accuracy of predictions from both predictors. The performance map of predictions obtained by ANN and persistence, in terms of nRMSE, are presented respectively in figure 5 and figure 6. We can

firstly observe that the nRMSE stay between 14 % and 24 % for a wide majority of pixels in both cases . Predictions performances maps are comparable, since the spatial distribution of nRMSE$_{ANN}$ and nRMSE$_{persist}$ values are quite similar : for both maps, nRMSE have lower values over the sea and the center of the island and higher values over its seaside parts, especially around the oriental coast. Thus, we can notice that predictions performances seem correlated with local topography since best predictions correspond to mountainous area (Fig. 1). The predictions over these zones seems to be easier since the weather variability and dynamics might be less fast than over the coasts
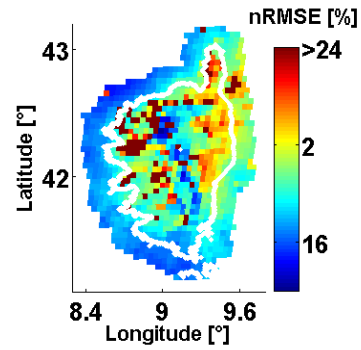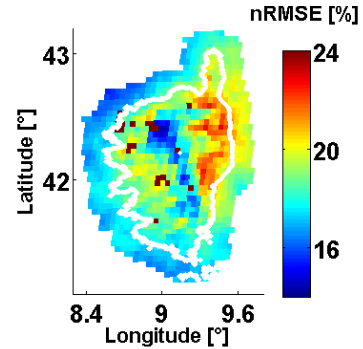

Figure 5: nRMSE$_{ANN}$ map (nRMSE for ANN)

Figure 6: nRMSE$_{persist}$ map (nRMSE for the persistence)

Besides, more pixels have nRMSE$_{ANN}$ > 24 % (hitting punctually 34 %) but globally, the persistence and the ANN has same performances since their spatial mean of nRMSE are both 18.5 %. However, a majority of points have nRMSE$_{persist}$ > nRMSE$_{ANN}$ (Fig. 7).
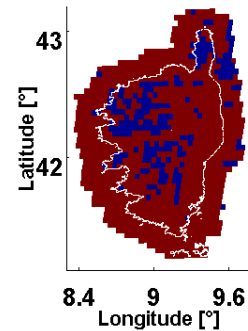

Figure 7: map representing pixels were nRMSE$_{persist}$ > nRMSE$_{ANN}$. (In red: nRMSE$_{persist}$ > nRMSE$_{ANN}$ - In blue: nRMSE$_{persist}$ < nRMSE$_{ANN}$.)

Thus, despite an equivalent global nRMSE, the ANN

used to have best performances than persistence. Actually, MLP of a few pixels present clearly worst performances than persistence whereas the pixel of best performances have very closed nRMSE. In fact, ANN interest is not obvious for this application, all the more so it necessites much more parameters than a persistence that offers comparable even best results.

5   CONCLUSIONS

The possibility to generate 2-D predictions of solar radiation over Corsica is explored in that paper. In that view, satellite derivate SSI from HelioClim-3 database are used as inputs of two types of predictors: Artificial Neural Networks and scaled persistence.

Comparisons between satellite estimated SSI maps and prediction maps show that predictions are more accurate over the inner island than over the coasts. Besides, MLP and persistence present similar performances for a wide majority of pixels. Thus, The relevance of ANN usage in that application is not obvious, especially if we consider the Occam's razor principle that favor the simplest theory among theories that give similar results. .

Yet, the SSI maps offer a new opportunity to predict solar radiation in another way. We can use spatial weather behavior rather than its temporal one. Actually, the idea would be to use solar radiation of points around the studied pixel at time t to predict it radiation at t + 1.

6   REFERENCES

[1] Voyant, C., 2011. Prédiction de séries temporelles de rayonnement solaire global et de production d'énergie photovoltaïque à partir de réseaux de neurones artificiels. PhD Thesis, university of Corsica.

[2] Haurant, P., 2012. De la sélection multicritère de parcs photovoltaïques à la cartographie et l'étude de l'intermittence de la ressource : modélisations appliquées à l'île de Corse. PhD Thesis, universiy of Corsica

[3] Voyant, C., Muselli, M., Paoli, C., et Nivet, M., 2011. Optimization of an artificial neural network dedicated to the multivariate forecasting of daily global radiation. Energy, 36(1), 348–359.

[4] Voyant, C., Muselli, M., Paoli, C., Nivet, M.-L., 2012. Numerical weather prediction (NWP) and hybrid ARMA/ANN model to predict global radiation. Energy 39, 341–355.

[5] Rome S, and Giorgetti J. La montagne corse et ses caractéristiques climatiques. La Météorologie 2007; 59.

[6] Rodriguez, E., Morris, C., Belz, J., Chapin, E., Martin, J., Daer, W., et Hensley, S. (2005). An Assessment of the SRTM Topographic Products. (Rapport technique). Pasadena, California : Jet Propulsion Laboratory.

[7] Haurant, P., Muselli, M., Pillot, B., Oberti, P., 2012. Disaggregation of satellite derived irradiance maps: Evaluation of the process and application to Corsica. Solar Energy 86, 3168–3182.

[8] Blanc, P., Gschwind, B., Lefèvre, M., Wald, L., 2011. The HelioClim Project: Surface Solar Irradiance Data for Climate Applications. Remote Sensing 3, 343–361.

[9] Rigollier, C., Lefèvre, M., etWald, L., 2004. The method Heliosat-2 for deriving shortwave solar radiation from satellite images. Solar Energy, 77(2), 159–169.

[10] Rigollier, C., Bauer, O., et Wald, L., 2000. On the clear sky model of the ESRA – European Solar Radiation Atlas – with respect to the Heliosat method. Solar Energy, 68(1), 33–48.

[11] Mellit, A., Kalogirou, S.A., Hontoria, L., Shaari, S., 2009. Artificial intelligence techniques for sizing photovoltaic systems: A review. Renew. Sustain. Energy Rev. 13, 406–419